

Towards an AI-enabled Connected Industry: AGV Communication and Sensor Measurement Datasets

Rodrigo Hernangómez*, Alexandros Palaios[§], Cara Watermann[§], Daniel Schäufele*, Philipp Geuer[§], Rafail Ismayilov*, Mohammad Parvini[†], Anton Krause[†], Martin Kasparick*, Thomas Neugebauer[¶], Oscar D. Ramos-Cantor[‡], Hugues Tchouankem[‡], Jose Leon Calvo[§], Bo Chen**, Sławomir Stańczak*^{||}, Gerhard Fettweis[†]

*Fraunhofer Heinrich Hertz Institute, Germany, {firstname.lastname}@hhi.fraunhofer.de

[§]Ericsson Research, Germany, {alex.palaios, cara.watermann, philipp.geuer}@ericsson.com

[†]Vodafone Chair, Technische Universität Dresden, Germany, {mohammad.parvini, anton.krause, gerhard.fettweis}@tu-dresden.de

[‡]Corporate Research, Robert Bosch GmbH, Germany, {oscardario.ramoscantor, huguesnarcisse.tchouankem}@de.bosch.com

^{||}Network Information Theory Group, Technische Universität Berlin, Germany

[¶]Götting KG, Germany, neugebauer@goetting.de

**Enway GmbH, Germany, bo@enway.ai

Abstract—This paper presents two wireless measurement campaigns in industrial testbeds: industrial Vehicle-to-vehicle (iV2V) and industrial Vehicle-to-infrastructure plus Sensor (iV2I+). Detailed information about the two captured datasets is provided as well. iV2V covers sidelink communication scenarios between Automated Guided Vehicles (AGVs), while iV2I+ is conducted at an industrial setting where an autonomous cleaning robot is connected to a private cellular network. The combination of different communication technologies, together with a common measurement methodology, provides insights that can be exploited by Machine Learning (ML) for tasks such as fingerprinting, line-of-sight detection, prediction of quality of service or link selection. Moreover, the datasets are labelled and pre-filtered for fast on-boarding and applicability. The corresponding testbeds and measurements are also presented in detail for both datasets.

Index Terms—Measurement data, QoS prediction, AGV, drive tests, V2X, campus networks, wireless communications

I. INTRODUCTION

It is anticipated that the next generation of wireless communication systems (5G and beyond) will bring about an upsurge in the number of new services and applications; each of which demanding for a specific Quality of Service (QoS). In parallel, there is a resurgence of interest in promoting the concept of predictive Quality of Service (pQoS), i.e., QoS estimation for a given time instance in the future. This can be done in different prediction horizons, ranging from milliseconds to hours or even days. pQoS can pave the way to satisfy a very demanding set of QoS requirements, e.g., very low latency, minimum Signal-to-Noise Ratio (SNR), delay, packet error rate, or huge Uplink (UL) or Downlink (DL) throughput.

pQoS can be particularly important for wireless networks in the industrial domain, where communication needs to be highly reliable due to, among other reasons, its integration into

control loops. Wireless links are especially relevant in mobile setups, e.g., with one or more Automated Guided Vehicles (AGVs) connected in a Vehicle-to-vehicle (V2V), Vehicle-to-infrastructure (V2I) or Vehicle-to-everything (V2X) manner. In this regard, some datasets are available for automotive scenarios to train and test Machine Learning (ML) algorithms and thus enhance such schemes [1]. However, the availability of datasets from industrial and indoor measurement campaigns, such as [2], is limited. With proper knowledge of the upcoming QoS conditions, pQoS can facilitate the proper operation of industrial applications to guarantee human-machine safe interaction or robot cooperation to fulfill a common task. Other use cases may include tele-operated driving, high-density platooning, and High Definition (HD) map collecting and sharing for optimal route selection [3], [4].

In this manner, we can see a growing tendency toward applying deep learning algorithms for pQoS applications, such as [5]–[8], to name a few. A consolidated overview of the ML-enabled throughput prediction scenarios is presented in [5]. In the same vein, [6] investigates a ML-model to predict the throughput in a non-standalone 5G network.

ML has been a very active research area in the past few years and there is ample literature around it; however, its real-world implementation or validation has remained elusive for industrial communication due to its high dependency on available datasets to test, validate and generalize the algorithms. Therefore, creating a reference dataset from experimental testbeds or practical simulations is paramount to evaluate the underlying theoretical models.

In this paper, we will describe the industrial Vehicle-to-vehicle (iV2V) dataset and the industrial Vehicle-to-infrastructure plus Sensor (iV2I+) dataset. These two datasets aim to pave the way for future advancement in the experimentation of mobile networks. The measurement campaigns that were conducted here are part of a bigger measurement framework and procedure that is described in detail in [9]

This work was supported by the Federal Ministry of Education and Research (BMBF) of the Federal Republic of Germany as part of the AI4Mobile project (16KIS1170K). The authors alone are responsible for the content of the paper.

with some first results being reported in [10].

The remainder of this paper is structured as follows. In Section II and Section III, we describe the iV2V and iV2I+ testbed and datasets and we elaborate on their details and components. We conclude with an overview of possible future research directions in Section IV.

II. THE iV2V TESTBED AND DATASET

In this section, we present the first of the two collected datasets and the considerations that have been taken into account for its measurement campaign. We give a brief introduction to the sidelink technology, continue with a detailed description of the testbed, and finally describe the processing and resulting data structures.

Figure 1a depicts one of the AGVs, carrying the measurement and communication hardware. The AGVs communicate directly in a V2V manner, using the sidelink technology as introduced by 3rd Generation Partnership Project (3GPP) in Release 14. In the sidelink setup, every AGV acts both as transmitter and sender (c.f. Figure 1b).

A. Testbed Components

1) *Sidelink*: Sidelink has been standardized in 3GPP during 4G and 5G mobile networks to define a framework where communication is possible with and without network coverage and with varying degrees of interaction between the devices and the network. Two modes of resource allocation are defined [11]:

- *Network-based resource allocation (Mode 1 in 5G sidelink and Mode 3 in 4G sidelink)*: This mode is only available when all the devices are in network coverage, and the network selects the resources and other transmit parameters used by the devices.
- *Autonomous resource allocation (Mode 2 in 5G sidelink and Mode 4 in 4G sidelink)*: This mode offers a completely decentralized solution in which the User Equipments (UEs) autonomously select the resources and other transmit parameters.

Overall, network-based resource allocation can outperform the autonomous case. This is due to the network controlling the resources to be used by each of the UEs involving UL signaling from the UE to the network to obtain a grant for transmissions [12].

On the other hand, autonomous resource allocation is mainly useful when there is no possibility of having network coverage. The basic operation of autonomous resource selection involves the device performing sensing within a pre-configured resource pool, detecting which resources are not in use by other devices with higher-priority traffic, and choosing some of these free resources for its transmissions [12]. The autonomous resource allocation is more prone to collisions while also suffering from hidden node and half duplex problem. Solutions have been considered in 3GPP to mitigate these issues [13].

For the measurement campaign, we use a full stack, software-based, standard-compliant and open implementation

of the 3GPP Release 14 PC5 Mode 4 standard [14]. The platform allows research concepts and standard features to be validated in hardware testbeds and it provides interfaces and tools for recording measurement data. Changes and adjustments are possible at every layer, which allows a realistic verification of new features. The sidelink software (all layers incl. baseband processing) can be run on standard general purpose computing hardware in connection with suitable Software Defined Radio (SDR) hardware. We opted for a full stack implementation, thus providing a standard based IP to IP (one to all) interface for any application, i.e., all protocols on OSI layer 3 and higher can be transferred. The hardware setup is shown in Figure 1c (cf. [14] for further details).

2) *Localization*: Precise position of the communicating devices is required to link the environmental conditions with the measured data. For that purpose, the position information provided by the AGVs, carrying the communication entities, was recorded during the measurements. Two types of localization methods are used by different AGVs in the testbed, namely, marker/track-based, and Simultaneous Localization and Mapping (SLAM)-based. In the former method, the AGVs follow a track on the floor with help of an onboard camera. Additionally, Radio-frequency identification (RFID) tags are placed on the track to provide the exact position information to the AGVs, when they pass over. Between the RFID tags, the AGVs estimate their position by using odometry, which describes a method of estimating the position and orientation of a mobile system using data from its propulsion system. Wheel-driven systems use the measurement of the wheel rotations for this. In combination with dead reckoning, odometry is a basic navigation method for ground-based vehicles. Since the AGVs do not leave the track, the transversal error is in the order of few mm, while the longitudinal error depends on the separation distance between the RFID tags and the positional accuracy.

For our testbed, the longitudinal error was in the order of few cm. In the latter localization method, i.e., SLAM-based, the AGVs are equipped with a laser scanner to detect and estimate the distance to landmarks (reference points) in the testbed. These landmarks are also defined in the map of the AGV system. Hence, the AGVs can estimate their position in the map through a combination of information from several landmarks. In the testbed, we achieve a position accuracy in the order of few cm with the SLAM-based method.

The reported AGV position was timestamped during the measurements, so that a combination with other measured data is possible during post-processing. Unless otherwise stated, the measurements scenarios presented below consider that the SLAM-based AGVs were static and the marker/track-based AGVs were moving.

Since the moving AGV is guided by an optical line, the real lateral position is better than ± 2 mm (3σ). The along track (longitudinal) error while passing an RFID tag has a timing uncertainty of up to 30 ms, which gives an error depending on the actual speed (up to 30 mm at 1m/s). Dead reckoning results in additional errors being displayed due to the route

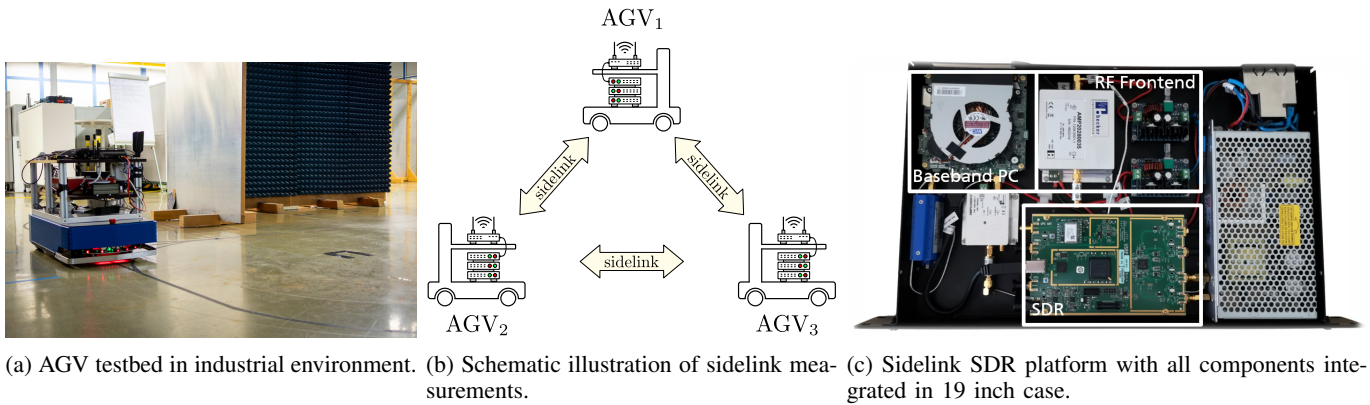


Fig. 1: iV2V testbed.

and steering angle sensors not being perfectly adjusted. The longitudinal error increases with the length of the unsupported route driven without an RFID tag. The repeatability of the position information is less than ± 2 mm transversally and less than $+2$ cm longitudinally at the driven speed.

3) *Time Synchronization*: To enable accurate evaluation of network latency and other QoS properties, a proper time synchronization is required. The time was synchronized across sidelink devices by running NTP over Ethernet. The error is typically in the order of several μ s with a worst case error of 1 ms. However, precisely quantifying this is difficult without specialized measurement equipment.

4) *Controlled Packet Generation*: To ensure a highly precise packet generation, we used a network packet generator tool based on Real-time User Datagram Protocol (UDP) Data Emitter (RUDE) & Collector for RUDE (CRUDE) which is able to produce heterogeneous UDP network traffic for realistic network workloads [15]. It consists of two main modules: RUDE generates traffic to the network, which is then received and logged by the other module of the network with CRUDE. We extended the packet generator tool by enabling the capability to log all channel information for successfully received packets.

5) *Automatic Gain Control*: In order to be able to assess the received signal quality, which is an elementary quantity for assessing the QoS, the function of the Automatic Gain Control (AGC) in a receiver must be understood. AGC is a feature in an RF receiver signal path that is used to keep the received signal magnitude at a suitable level for subsequent signal processing so that signals are not clipped and the receive path with good sensitivity is operated. The function of the AGC is technically realized by controllable amplifiers in the received signal path. For this purpose, the signal level is determined in the signal processing during special preambles at the beginning of a defined data frame and regulated within a specified range by setting the AGC. A criterion for the regulation can be the evaluation of the preamble of the Orthogonal Frequency-Division Multiplexing (OFDM)-based signal obtained from the I/Q samples. However, the corresponding values at the antenna input, namely Received Signal Strength Indicator

(RSSI) and Reference Signal Received Power (RSRP), are of interest for signal evaluation and a corresponding indication of comparable level values. With knowledge of the amplification and attenuation of individual components in the front-end and the AGC setting, these can be determined from the measured values, i.e. from the total gain between the antenna input and the evaluation stage. The AGC calculations have already been performed before the output and the values supplied for pre-processing are the correct values and can be used as is.

B. Measurement Scenarios

We collected data for roughly 10 hours over the course of two days to acquire almost 50 GB communication data between up to three industrial AGVs. A schematic of the test area and its surroundings is presented in Fig. 2. The dotted gray line depicts the track used by AGV 1. Several obstacles, depicted in different blue tones in the figure, were located within the test area to achieve different radio propagation conditions, e.g., Line-of-Sight (LOS) and Non-Line-of-Sight (NLOS) conditions. The obstacles were rearranged during the measurement campaign to create two scenarios, A and B, with different N/LOS characteristics, as marked in light blue in the figure.

C. The Dataset

1) *Captured Sidelink Data*: For each scenario illustrated in Figure 2, we capture the sidelink channel parameters for every transmitter/receiver pair. The selected sidelink channel parameters and their description are presented in Table I. The parameters in the table are obtained/estimated from the Demodulation Reference Signal (DMRS) of the Physical Sidelink Shared Channel (PSSCH).

The AGV localization data is provided as x and y coordinates in a local coordinate system.

2) *Dataset Pre-processing*: In this section, we describe the pre-processing of captured sidelink data, and we present a dataset constructed with the pre-processed data. The dataset is constructed in a tabular format where each row represents a sample and the columns contain the value of the measured sidelink channel parameters. Note that the side channel

A. Testbed Components

The testbed for the measurements is located in an industrial co-working space in Berlin, with a layout as shown in Fig. 3c. The hall had a gateway, which allowed the AGV to drive outside.

1) *The AGV*: The AGV used in the testbed is an autonomous cleaning robot from the company Enway, as shown in Fig. 3a. They are specially designed for use under the operating conditions of the manufacturing industry.

The sweeper has all the necessary navigation data saved on a digital map, and drives over the cleaning area autonomously. Thanks to high-performance sensors and control software from Enway, the AGV navigates the environment completely independently. Using a combination of laser distance measurement and cameras, the robot captures the environment in three dimensions. This 360-degree view enables very safe navigation between people, complex production lines, and overhanging systems. The AGV immediately detects obstacles that suddenly appear along the route, and drives around them. Additional equipment such as floor markings, QR codes, or magnetic tracks are not required for navigation. In the event that the AGV encounters an unsolvable situation, the robot stops and reports automatically to Enway headquarters via a data connection. The remote team monitors every movement of the device around the clock. The specialists can end autonomous journeys at any time, and can take control from a distance. Collisions with people, production systems, vehicles, and stored goods are thus avoided at all times. The machine can also be navigated manually by the operating personnel on site, if necessary. Because the AGV is a retrofitted ride-on sweeper, it can be controlled from the driver's seat in the traditional sense. Ongoing use of the autonomous sweeper can be monitored, controlled, and then evaluated using mobile devices such as smartphones, laptops, or tablets. The software completely logs the cleaning trips.

2) *Cellular Network*: The mobile network used for the measurements in this test bed corresponded to a standardized 4G campus network with TDD medium access. The bandwidth was 20 MHz in the frequency band between 3700 and 3800 MHz approved by the Federal Network Agency. A corresponding frequency assignment was applied for the period of the measurements. The hardware consisted of a server running the LTE core and a radio base station with integrated antennas connected to the server via Gbit LAN and powered via Power over Ethernet (PoE). The location of the base station is marked in Fig. 3c with a yellow circle. A Mini-PC with the Linux operating system was used as the UE to carry out QoS-relevant measurements on the AGV. A Quectel RM500Q-GL card was used as the radio device, which was connected to the Mini-PC via USB. External antennas were connected to the radio.

The server provides a service interface to which the applications required for the measurements can be connected. The stationary applications can communicate with mobile applications running in the Mini-PC via the service interface. This

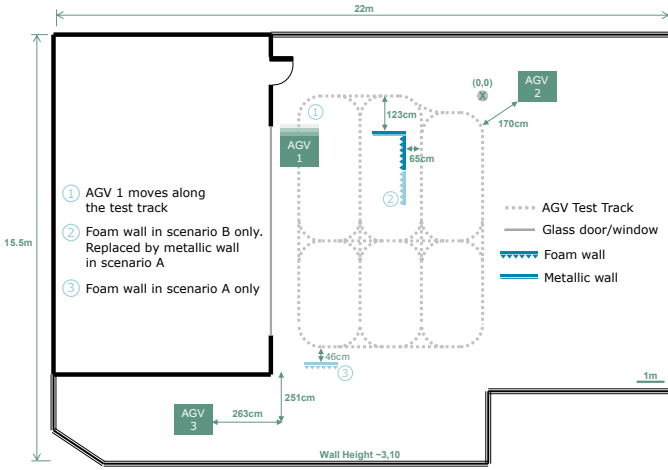


Fig. 2: Illustration of measurement scenarios A & B.

TABLE I: Selected iV2V Data Features.

Parameter	Description
SNR [dB]	Derived from noise and power estimations of DMRS
RSRP [dBm]	Average energy per carrier/RE for DMRS
RSSI [dBm]	Signal power over the whole band
Noise Power	Estimated on DMRS in decoded subframe
Time [sec]	Receive time of first IQ-Sample of decoded subframe
Frame Number	System frame number
Subframe Number	System subframe number
UHD Rx Gain [dB]	Receive antenna gain
SCI FRL N	Starting subchannel of decoded PSSCH
SCI FRL L	Number of used subchannels for PSSCH
RLC SN	Sequence number of radio link control header
Location	Local x and y coordinates of AGV 1 on the track

parameters and AGV location are measured independently and simultaneously in different devices. With this setting, each measuring device embeds its own timestamp into the measured parameters. Since the processing of the received signal in different devices requires different lengths of time, the embedded timestamps in these devices also have some differences. We align the timestamps between the location data and the sidelink data as follows. Given the timestamp t_n^{loc} corresponding to the measured location $\mathbf{L}_n = [x_n, y_n]$ of the AGV at n^{th} time step, we find the timestamp t_n^{sl} from the measured sidelink such that $|t_n^{\text{loc}} - t_n^{\text{sl}}| \leq \gamma$, where γ denotes the alignment tolerance, and we use $\gamma = 0.005\text{s}$ to construct the dataset.

In addition, we present indicators $M_n \in \mathbb{Z}$ and $S_n \in \mathbb{Z}$, where M_n indicates the measurement scenario (i.e., the placement of obstacles), and S_n denotes the source of the received sidelink signal (i.e., AGV₁ receives a signal from AGV₂ or from AGV₃). With the parameters described in Table I, the n^{th} row of the tabular dataset is denoted by \mathbf{R}_n , and it contains the parameters as $\mathbf{R}_n = [t_n^{\text{loc}}, t_n^{\text{sl}}, |t_n^{\text{loc}} - t_n^{\text{sl}}|, \mathbf{L}_n, \mathbf{P}_n, S_n, M_n]$, where $\mathbf{P}_n \in \mathbb{R}^K$ denotes the K measured parameters of sidelink channel.

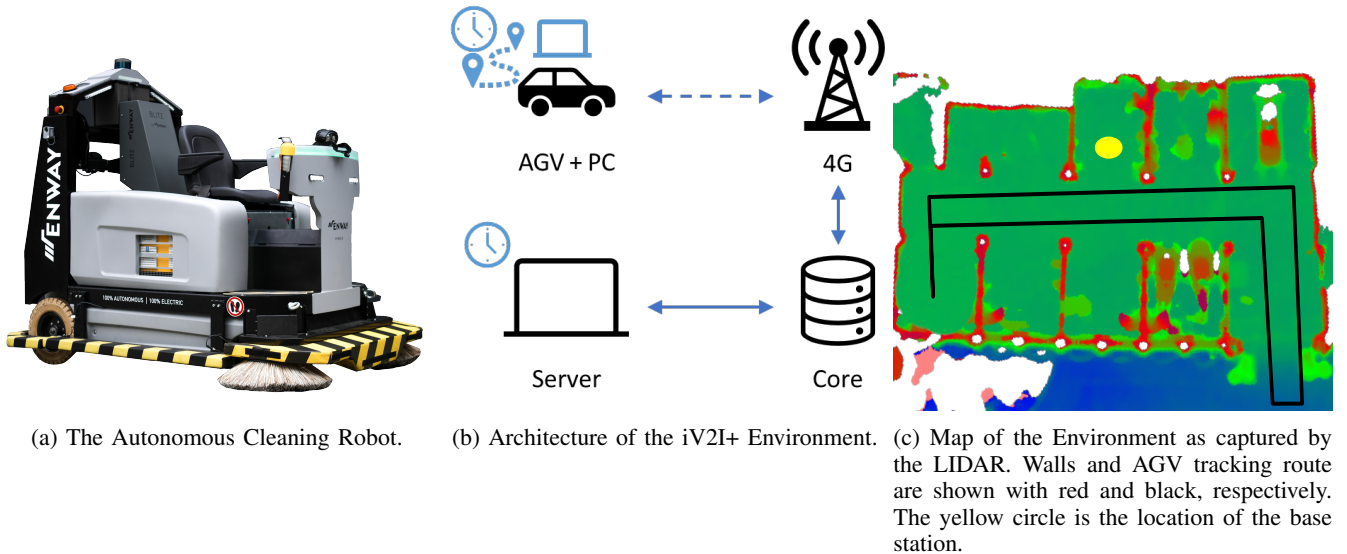


Fig. 3: iV2I+ testbed.

way, the location-dependent data rate and latency parameters relevant for evaluating the QoS can be determined at the Mini-PC.

3) *Time Synchronization*: The AGV and the server were time synchronized. Fig. 3b visualizes the communication set-up, where the dotted arrow shows the wireless connection and the solid line the cable connection. Both the server and the Mini-PC on the AGV were connected to a GPS receiver, allowing accurate time synchronization by using Pulse-per-Second (PPS) signal. The maximum error is typically in μ s-range. However, the AGV only had consistent GPS reception at the start point and the outdoor area, which could lead to inaccuracies the ms-range.

4) *LTE Modem Access*: We used Mobile Insight, an open-source cross-platform application for mobile network monitoring and analytics to capture mobile network data at the Mini-PC. It collects mobile network information across several cellular protocols, e.g. Radio Resource Control (RRC) or EPS Mobility Management (EMM). During the measurement campaign, the available information was logged every 40 ms.

Additionally, a Python script that accesses the modem via a virtual serial interface, a few radio parameters (RSSI, RSRP, Reference Signal Received Quality (RSRQ), Signal-to-Interference-plus-Noise Ratio (SINR)) were logged every 200 ms by the modem and written to a file with a time stamp. The data can then be linked to other data, e.g. the location, via the common time stamps.

5) *Controlled Packet Generation*: We used the application iperf3 on the Mini-PC and the server to generate UDP traffic in either UL or DL direction. Apart from the generated iperf3 log files, tcpdump was used both on the Mini-PC and server to capture all incoming and outgoing packets at the respective network interfaces, allowing a more detailed evaluation on a packet level.

B. Measurement Scenarios

For the measurement campaign, one AGV, equipped with the sensors and measurement devices described in the prior section, was driving through the testbed area over the course of three days. Overall, 16 hours of data were collected.

UL and DL communication was measured. Two types of packet flows were established to generate high and medium throughput. In DL, high throughput measurements were conducted with a throughput target of 80 Mbps, in UL with 25 Mbps. Approximately twice as many high throughput measurements as medium throughput measurements were collected. The route contained a diverse set of radio conditions, namely: LOS and NLOS situations, coverage loss as well as indoor and outdoor measurements. The measured path is shown in Fig. 3.

C. The Dataset

For each scenario, data from the described network components and the sensors from the AGV was collected. A subset of the captured data is presented in Table II.

TABLE II: Selected iV2I+ Data Features.

Parameter	Description
SINR [dB]	Derived from noise and power estimations of DMRS
RSRP [dBm]	Average energy per carrier/RE for DMRS
RSSI [dBm]	Signal power over the whole band
Throughput	Acquired throughput in respective link direction
Ping [ms]	Time in ms until a ping reply was received
Jitter	Delay variation measured over 1s
Odometry	Fused position, orientation and speed of the AGV
Map static elevation	Single pre-computed map of the whole area
Near/far map obstacles	36 m ² /400 m ² obstacle map around the AGV
LIDAR	3D point cloud with obstacles

1) *AGV-Sensor Data*: The AGV delivers a series of sensor data via its Robot Operating System (ROS), including the last four rows in Table II. Except for Light Detection and Ranging (LIDAR), all ROS topics shown here are obtained through

sensor fusion (e.g., through techniques such as Extended Kalman Filter (EKF)) and provide the relevant information from a wireless perspective: position, orientation and speed of the AGV and location of walls and obstacles in different formats (2D, 3D, offline and online, near and far). The raw input for the sensor fusion comes from sources including pure wheel odometry, drive commands, an Inertial Measurement Unit (IMU) and the already mentioned LIDAR, all of them also available in the dataset.

D. Pre-Processing

Similar to what was described in Section II-C2 the data was pre-processed to further simplify the work with the collected data. Moreover, and since the position of the base station is known and fixed, the distance and clearance of the wireless link can be easily inferred from the sensor data and is provided as part of the pre-processed dataset.

We have merged the GPS logs, the LTE stack measurements and the throughput measurement together with the sensor-based link distance and link clearance into a single dataframe. As these data streams have different sampling frequencies, we re-sampled as needed to 1 second before the final merge.

IV. CONCLUSION

In this paper, we have describe industrial Vehicle-to-vehicle (iV2V) and industrial Vehicle-to-infrastructure plus Sensor (iV2I+), two testbeds for wireless communications in industrial settings. We have provided detailed information about the components of the testbeds, together with the initial concept and captured scenarios. As mentioned before, the described datasets are publicly available for ML research, what we consider a valuable contribution to the available industrial datasets both in terms of size and quality.

iV2V and iV2I+ contain extensive and complete data that we believe to be highly useful to answer questions regarding the use and generalisation of ML for mobile use cases in industrial environments. Indeed, both datasets can be used to train and evaluate methods for pQoS, which is a crucial enabler for high reliability in wireless industrial applications. Moreover, pQoS in general, and our data in particular can be used as an ingredient for ML algorithms that optimize the network itself, e.g., by performing proactive radio resource management (RRM). This type of new network capabilities will be an important part of the evolution of wireless communications, such as the 6G cellular evolution. Finally, the addition of AGV sensor data and localization opens the gate to advanced techniques like fingerprinting or channel charting.

REFERENCES

- [1] D. Schäufele, M. Kasparick, J. Schwardmann, J. Morgenroth, and S. Stańczak, "Terminal-side data rate prediction for high-mobility users," in *2021 IEEE 93rd Vehicular Technology Conference (VTC2021-Spring)*. IEEE, 2021, pp. 1–5.
- [2] F. Burmeister, Z. Li, and I. Bizon, "High-Resolution Radio Environment Map Data Set for Indoor Office Environment," 2022. [Online]. Available: <https://dx.doi.org/10.21227/waxd-9525>
- [3] M. Boban, M. Giordani, and M. Zorzi, "Predictive Quality of Service: The Next Frontier for Fully Autonomous Systems," *IEEE Network*, vol. 35, no. 6, pp. 104–110, Dec. 2021.
- [4] D. F. Külzer, M. Kasparick *et al.*, "AI4Mobile: Use cases and challenges of AI-based QoS prediction for high-mobility scenarios," in *Proc. IEEE Vehicular Technology Conference (VTC Spring)*, Apr. 2021, pp. 1–7.
- [5] D. Raca *et al.*, "On leveraging machine and deep learning for throughput prediction in cellular networks: Design, performance, and challenges," *IEEE Communications Magazine*, vol. 58, no. 3, pp. 11–17, Mar. 2020.
- [6] D. Minovski *et al.*, "Throughput prediction using machine learning in LTE and 5G networks," *IEEE Transactions on Mobile Computing*, 2021.
- [7] C. Luo *et al.*, "Channel state information prediction for 5G wireless communications: A deep learning approach," *IEEE Transactions on Network Science and Engineering*, vol. 7, no. 1, pp. 227–236, Jan.-Mar. 2018.
- [8] H. Ye, G. Y. Li, and B.-H. Juang, "Power of deep learning for channel estimation and signal detection in OFDM systems," *IEEE Wireless Communications Letters*, vol. 7, no. 1, pp. 114–117, Feb. 2018.
- [9] A. Palaios *et al.*, "Network under Control: Multi-Vehicle E2E measurements for AI-based QoS prediction," in *2021 IEEE 32nd Annual International Symposium on Personal, Indoor and Mobile Radio Communications (PIMRC)*, 2021, pp. 1432–1438. [Online]. Available: <https://ieeexplore.ieee.org/document/9569490>
- [10] —, "Effect of spatial, temporal and network features on uplink and downlink throughput prediction," in *Proc. IEEE 5G World Forum (5GWF)*, Oct. 2021, pp. 418–423.
- [11] "Overall description of Radio Access Network (RAN) aspects for Vehicle-to-everything (V2X) based on LTE and NR (Release 17)," 3GPP, TR 37.985.
- [12] "5G NR; Physical layer procedures for control," 3GPP, TS 38.213.
- [13] "New WID on NR sidelink enhancement," 3GPP TSG RAN Meeting #86, Sitges, Spain, document RP-193257, Dec. 2019.
- [14] R. Lindstedt *et al.*, "An Open Software-Defined-Radio Platform for LTE-V2X And Beyond," in *2020 IEEE 92nd Vehicular Technology Conference (VTC2020-Fall)*, 2020, pp. 1–5.
- [15] S. Saaristo and R. Prior. (2022) RUDE-CRUDE 0.70. Accessed on: 2022-10-27. [Online]. Available: <https://rude.sourceforge.net/>